Soliton energies in the standard map beyond the chaotic threshold

1987 J. Phys. A: Math. Gen. 20 6211

(http://iopscience.iop.org/0305-4470/20/18/021)

J. Phys. A: Math. Gen. 20 (1987) 6211-6221. Printed in the UK

Soliton energies in the standard map beyond the chaotic threshold†

K Furuya and A M Ozorio de Almeida

Instituto de Física, UNICAMP, Campinas, 13081 SP, Brazil

Received 9 April 1987

Abstract. The Birkhoff-Moser theorem guarantees the existence of an analytical reduction to its normal form of an area-preserving map in the neighbourhood of an unstable fixed point. The stable and unstable manifolds emanating from this point are then simply the images of the axes in the normal coordinates. For sufficiently high parameter values of the standard map, the series for the manifolds can be resummed into a closed form, providing good approximations to the first loops of the manifolds. We thus obtain simple approximations for a pair of homoclinic orbits for parameters where most orbits are chaotic.

The Frenkel-Kontorova model consists of an infinite sequence of equal springs and masses under the action of a periodic potential. The configuration where all the masses lie at the minima of the potential corresponds to the unstable fixed point of the standard map. A soliton or discommensuration, where one of the minima is missed, is represented by a homoclinic orbit. Using the normal form we calculate the soliton energy and its pinning energy. Good agreement is found with the pinning energy of Pokrovsky, obtained as a perturbation from the continuum approximation.

1. Introduction

The Frenkel-Kontorova model consists of an infinite number of equal springs, joining an infinite sequence of unit masses at the positions θ_i, acted on by the periodic potential

$$V(\theta_i) = \alpha(1-\cos\theta_i). \tag{1}$$

This is sketched in figure 1(a). The initial problem is to determine the equilibrium configuration for the position θ_i under the action of the potential and the elastic force, as shown in figure 1(b). In other words, we seek the configuration $\{\theta_i\}$, which minimises the energy

$$E(\{\theta_i\}) = \sum_i [\tfrac{1}{2}(\theta_{i+1}-\theta_i-a)^2 + V(\theta_{i+1})] \tag{2}$$

as a function of the length a of the free springs and α, the strength of the potential. Some of the many applications of the Frenkel-Kontorova model in solid state physics are reviewed by Bak (1982).

Aubry (1978) presented a new treatment of this problem based on two main ideas. The first is to treat the infinite system as the limit of a finite one with N masses and fixed boundary conditions, or more precisely a fixed distance between θ_1 and θ_N. Except for a constant, the energy is then given by

$$\Phi(\{\theta_i\}) = \sum_i \Phi_i = \sum_i [\tfrac{1}{2}(\theta_{i+1}-\theta_i)^2 + V(\theta_{i+1})]. \tag{3}$$

† Work supported by CNPq, Finep and FAPESP.

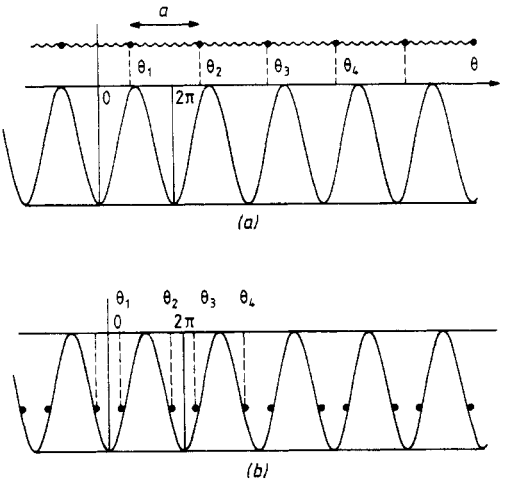

Figure 1. (*a*) Free chain with springs of length a and periodic potential $V(\theta) = \alpha(1 - \cos\theta)$; (*b*) minimum energy configuration for a chain where $a = \pi$. It is energetically favourable for the springs to be alternately stretched and compressed. This solution corresponds to a period-2 orbit in the standard map.

The second basic idea is now to treat Φ not as a static energy but as the action of a dynamical system with one degree of freedom and discrete time. The paths (θ_i, I_i) in two-dimensional phase space, for which the action Φ is stationary between θ_1 and θ_N, are exactly the trajectories of the dynamical system. These result from successive canonical transformations $(\theta_i, I_i) \rightarrow (\theta_{i+1}, I_{i+1})$, implicitly generated through the equations

$$I_{i+1} = \partial\Phi_i/\partial\theta_{i+1} \qquad I_i = -\partial\Phi_i/\partial\theta_i. \tag{4}$$

Each transformation then has the explicit form

$$\theta' = \theta + I \qquad I' = I + \alpha \sin(\theta + I) \tag{5}$$

recognised as the Taylor-Chirikov standard map.

The above identification is extremely useful because of the great amount of analytical and computational attention the standard map has received, as reviewed by Lichtenberg and Lieberman (1983). For $\alpha = 0$ the trajectories move along horizontal straight lines in phase space, corresponding to constant separation between the masses. These solutions are not pinned, i.e. we can translate the whole configuration by any $\Delta\theta$, thus obtaining an equivalent solution with the same energy. The KAM theorem implies that unpinned solutions, whose averaged rotations are incommensurate with the potential, continue to exist for small $\alpha > 0$. Beyond $\alpha \sim 1$, the chaotic threshold, there are no more unpinned solutions, the majority of the phase space being taken up by 'apparently random' orbits. For all α there are periodic solutions also. The simplest is the dynamically unstable fixed point at the origin, corresponding to placing all the masses at the potential minima. Another solution is the dynamically stable fixed point at $\theta = \pi$, corresponding to the statically unstable solution of placing all the masses on the crests of $V(\theta)$. In the latter case most points initially close to the fixed point remain in its neighbourhood, even though this is not a minimum energy configuration for the static chain.

The map orbits correspond to stationary energy configurations, but not necessarily to energy minima, as in the example above. In a remarkable series of papers (Aubry 1981, 1983a, b, Aubry and Le Daeron 1983, De Seze and Aubry 1984) Aubry and collaborators obtained conditions for minimising the energy of systems more general than the Frenkel-Kontorova model. It is there proved that unstable periodic orbits, corresponding to rotations of $n2\pi$, minimise the energy. Furthermore, homoclinic orbits, which tend to the periodic orbit for $i \to \pm\infty$, are also good solutions. In the continuum approximation, valid for $\alpha \to 0$, these solutions are known as solitons, though the appropriate term proposed by Aubry for the discrete system is discommensuration.

The homoclinic points are intersections of the stable manifold, a continuum of points which tends to the periodic orbit for $i \to \infty$, and the unstable manifold, similarly defined for $i \to -\infty$. Generally these manifolds intersect transversely in the standard map. Hence the solitons are pinned: we cannot translate the discommensuration by a lattice spacing without overcoming an energy barrier, even as $\alpha \to 0$. Pokrovsky (1981) was able to estimate the pinning energy in this limit for the soliton which accumulates on the unstable fixed point, as a perturbation from the continuum limit.

Our purpose is to apply analytical methods of finding homoclinic orbits to the calculation of the energy of this soliton and its pinning energy, beyond the chaotic threshold. The basis of these computations is the Birkhoff normal form (Birkhoff 1920) for the map in the neighbourhood of the unstable fixed point. Moser (1956) proved that the normal form converges in a neighbourhood of the fixed point and Ozorio de Almeida *et al* (1985) and Da Silva Ritter *et al* (1987) showed that the domain of convergence can actually extend far out along the stable and unstable manifolds, enabling the calculation of homoclinic points. After a preliminary discussion of homoclinic intersections and the definition of pinning energy in § 2, we present the method in § 3. A partial resummation of the series is possible, which leads to excellent approximations in closed form for the stable and unstable manifolds near a pair of homoclinic points. In § 4 we present computations of the soliton energy as well as the pinning energy. It is found that Pokrovsky's result can be extrapolated for parameters α, way beyond those for which his arguments hold, i.e. as far as $\alpha \sim 10$.

2. Homoclinic points and soliton energies

Figure 2 shows the homoclinic crossing of a pair of stable and unstable manifolds emanating from the unstable fixed points at $\theta = 0$ and 2π for $\alpha = 2$. These are calculated by placing many points very close to the origin on the linear approximation to the unstable manifold and iterating their orbits under the standard map. Likewise we place points on the stable manifold, which are then iterated under the inverse of the standard map:

$$\begin{aligned} \theta' &= -\theta + I + \alpha \sin\theta \\ I' &= I - \alpha \sin\theta. \end{aligned} \tag{6}$$

The loops of the unstable manifold become arbitrarily long as it returns to the neighbourhood of the fixed point at $\theta = 2\pi$, leading to many further intersections not shown here, corresponding to a pair of homoclinic orbits whose points alternate along both the stable and the unstable manifolds. These orbits have different energies, so that only the one with the lowest energy corresponds to the physical discommensuration.

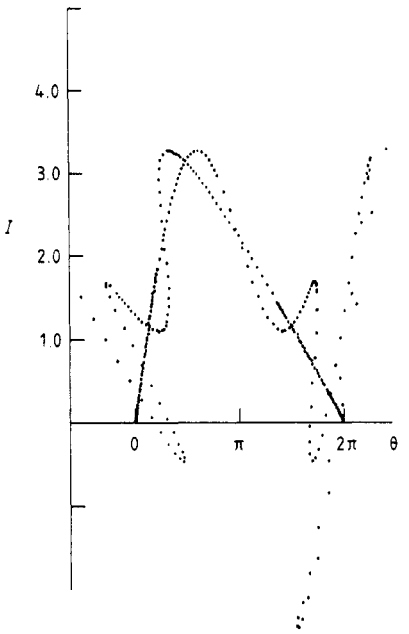

Figure 2. Homoclinic crossing of an unstable manifold leaving $\theta = 0$ and stable manifold arriving at $\theta = 2\pi$, obtained by iterating the map directly for $\alpha = 2$.

We can sort out the roles of the two homoclinic orbits by considering the symmetry about $\theta = \pi$ of the Frenkel-Kontorova problem. Though the map itself has no reflection symmetry about this line, the θ coordinates of the discommensuration must evidently be symmetric. We can consider the proper discommensuration as the limit of a long chain with N springs, such that the endpoints are fixed masses: $\theta_0 = 0$ and $\theta_N = 2\pi(N+1)$. The change in energy caused by the shift

$$\theta_i' = \theta_{i+1} \tag{7}$$

of all the masses, with the exception of the endpoints, tends to zero as $N \to \infty$. Let us consider the value of i for which θ_i is closest to π with $\theta_i < \pi$; then $\theta_{i+1} = 2\pi - \theta_i$. We can fix the ith mass in the chain at any point θ in the interval $(\theta_i, 2\pi - \theta_i)$. There results two subchains respectively with i and $(N-i)$ springs whose other endpoints are fixed at the origin and at $2\pi(N+1)$. The masses in between will arrange themselves so as to minimise separately the energy in each subchain. The total energy Φ is then a function of the single parameter θ. Placing θ at the maximum of the potential, $\theta = \pi$, the energy $\Phi(\pi)$ is obviously stationary with respect to θ. Since this energy is already minimal with respect to all other parameters θ_j, it follows that $\Phi(\theta = \pi)$ is the energy of a stationary configuration $\{\theta_j\}$, i.e. this is one of the two homoclinic orbits.

Evidently we minimise potential energy by avoiding the top of the $\theta = \pi$ barrier in the potential, so this solution does not correspond to the physical discommensuration. The energy $\Phi(\theta = \pi) = \Phi_m$ is the maximum in the continuous traversal from θ_i to $2\pi - \theta_i$. Thus, if Φ_s is the energy of the other homoclinic orbit, corresponding to the true discommensuration, we can define the pinning energy as

$$E_p = \Phi_m - \Phi_s \tag{8}$$

following Aubry (1983a, b).

3. Homoclinic points and the normal form

We can expand the standard map (5) in Taylor series about the origin, an unstable fixed point:

$$\begin{aligned} \theta' &= \theta + I \\ I' &= \alpha\theta + (1+\alpha)I + \alpha \sum_{n=1}^{\infty} \frac{(-1)^n}{(2n+1)!}(\theta + I)^{2n+1}. \end{aligned} \tag{9}$$

The linear part is now diagonalised by means of the linear canonical transformation

$$\begin{aligned} X &= I - (\lambda^{-1} - 1)\theta \\ Y &= I - (\lambda - 1)\theta \end{aligned} \tag{10}$$

where

$$\lambda = (1 + \alpha/2) + [(\alpha/2)^2 + \alpha]^{1/2} \tag{11}$$

is an eigenvalue of (9) and λ^{-1} is the other one. The transformed map thus becomes

$$\begin{aligned} X' &= \lambda X + \alpha \sum_{n=1}^{\infty} \frac{(-1)^n}{(2n+1)!(\lambda - \lambda^{-1})^{2n+1}} (\lambda X - \lambda^{-1} Y)^{2n+1} \\ Y' &= \lambda^{-1} Y + \alpha \sum_{n=1}^{\infty} \frac{(-1)^n}{(2n+1)!(\lambda - \lambda^{-1})^{2n+1}} (\lambda X - \lambda^{-1} Y)^{2n+1}. \end{aligned} \tag{12}$$

According to Birkhoff (1920) there exists a canonical non-linear transformation given by the formal Fourier series

$$\begin{aligned} X &= \xi + \sum_{k=2}^{\infty} \sum_{l=0}^{k} x_{kl} \xi^{k-l} \eta^l \\ Y &= \eta + \sum_{k=2}^{\infty} \sum_{l=0}^{k} y_{kl} \xi^{k-l} \eta^l \end{aligned} \tag{13}$$

such that the map in the (ξ, η) variables takes the simple form

$$\begin{aligned} \xi' &= U(\xi\eta)\xi \\ \eta' &= [U(\xi\eta)]^{-1}\eta \end{aligned} \tag{14}$$

Table 1. Numerical computation of homoclinic points from the full normal form.

α	$I_-/2\pi$	$\theta_-/2\pi$	$I_+/2\pi$	$\theta_+/2\pi$
1.0	0.337 814 094	0.330 945 436	0.282 816 720	0.507 164 126
2.0	0.500 463 215	0.249 188 126	0.355 829 181	0.500 010 055
3.0	0.606 434 800	0.196 783 198	0.390 334 334	0.499 996 923
4.0	0.675 949 305	0.162 021 080	0.411 084 837	0.500 000 368
5.0	0.724 181 488	0.137 910 662	0.425 051 327	0.500 000 070
6.0	0.760 678 109	0.118 893 792	0.435 133 358	0.500 000 101
7.0	0.800 778 759	0.090 329 620	0.442 775 775	0.500 000 082
8.0	0.811 845 553	0.091 716 110	0.448 778 723	0.500 000 022
9.0	0.826 834 139	0.085 790 016	0.453 624 171	0.500 000 011

where the function U takes the formal series expansion

$$U(\xi\eta) = \lambda\left(1 + \sum_{k=1}^{\infty} U_{2k}(\xi\eta)^k\right). \tag{15}$$

Since U depends only on the product $\xi\eta$, we can multiply both equations (14), obtaining

$$\xi'\eta' = \xi\eta. \tag{16}$$

The square hyperbolae $\xi\eta$ = constant are therefore open invariant curves of the Birkhoff map, just as XY = constant are invariant curves of the linear approximation to (12). The ξ axis and the η axis map respectively onto the unstable and the stable manifolds of the fixed point at the origin of the standard map (5).

Birkhoff did not establish the convergence of the formal series (13) and (15). Indeed, the corresponding series for a stable fixed point are known to be divergent. However, Moser (1956) did prove convergence of these series in a disc surrounding the origin, with the condition that the series (12) represent an analytic function, as in this case. In other words, the Birkhoff-Moser theorem guarantees the existence of an analytical transformation (13), taking the (standard) map into (14), where U is an analytic function of the product $\xi\eta$. Da Silva Ritter *et al* (1987) showed that if the inverse map is also analytic, as in (6), then the region of convergence of the series in fact extends indefinitely far out in a narrow strip along the stable and unstable manifolds, though the width of the strip narrows exponentially. Computations presented there for a quadratic family of maps confirm earlier results of Ozorio de Almeida *et al* (1985) that the Birkhoff normal form provides an excellent basis for the calculation of homoclinic points.

Defining the auxiliary series

$$(\lambda X - \lambda^{-1}Y)^{2n+1} \equiv Z^{2n+1} \equiv \sum_{k=2n+1}^{\infty}\sum_{l=0}^{k}(z^{2n+1})_{kl}\xi^{k-l}\eta^l \tag{17}$$

and introducing (13) into both sides of (12), we obtain the recurrence relations

$$\begin{aligned}\lambda U_{k-1}\delta_{k,2l+1} - \lambda x_{kl} &= \alpha \sum_{n=1}^{(k-1)/2} \frac{(-1)^n (z^{2n+1})_{kl}}{(2n+1)!(\lambda-\lambda^{-1})^{2n+1}} \\ &\quad -\lambda^{k-2l}\sum_{n=0} x_{k-2n,l-n}(U^{k-2l})_{2n} \\ \lambda (U^{-1})_{k-1}\delta_{k,2l-1} - \lambda^{-1} y_{kl} &= \alpha \sum_{n=1}^{(k-1)/2} \frac{(-1)^n (z^{2n+1})_{kl}}{(2n+1)!(\lambda-\lambda^{-1})^{2n+1}} \\ &\quad -\lambda^{k-2l}\sum_{n=0} y_{k-2n,l-n}(U^{k-2l})_{2n}\end{aligned} \tag{18}$$

where the last sum in both equations extends as far as $x_{k'l'}$ and $y_{k'l'}$ have non-negative indices. The unstable manifold is the image of the ξ axis given by the odd-powered series

$$X = \xi + \sum_{k=3}^{\infty} x_{k0}\xi^k \qquad Y = \sum_{k=3}^{\infty} y_{k0}\xi^k. \tag{19}$$

The recursion relations for x_{k0} and y_{k0} are independent of those for the other coefficients, taking the simple form

$$\begin{aligned} x_{k0} &= \frac{\alpha}{(\lambda^k - \lambda)} \sum_{n=1}^{(k-1)/2} \frac{(-1)^n (z^{2n+1})_{kl}}{(2n+1)!(\lambda-\lambda^{-1})^{2n+1}} \simeq \frac{(-1)^{(k-1)/2}\alpha\lambda^k}{k!(\lambda^k-\lambda)(\lambda-\lambda^{-1})^k}[1+O(\lambda^{-3})] \\ y_{k0} &= \frac{\alpha}{(\lambda^k - \lambda^{-1})} \sum_{n=1}^{(k-1)/2} \frac{(-1)^n (z^{2n+1})_{kl}}{(2n+1)!(\lambda-\lambda^{-1})^{2n+1}} \simeq \frac{(-1)^{(k-1)/2}\alpha\lambda^k}{k!(\lambda^k-\lambda^{-1})(\lambda-\lambda^{-1})^k}[1+O(\lambda^{-3})]. \end{aligned} \tag{20}$$

If we consistently neglect all terms of order λ^{-2} in the coefficients x_{k0} and y_{k0}, we can therefore resum the series (19) in the form

$$\begin{aligned} X &\approx (1-\alpha/\lambda)\xi + \alpha \sin(\xi/\lambda) \\ Y &\approx (-\alpha/\lambda)\xi + \alpha \sin(\xi/\lambda). \end{aligned} \tag{21}$$

Inverting the linear transformation (10), we thus obtain the approximate parametric equations for the unstable manifold as

$$\theta \approx \xi/\lambda \qquad I \approx [1-(\alpha+1)/\lambda]\xi + \alpha \sin(\xi/\lambda). \tag{22}$$

The stable manifold is the image of the η axis

$$X = \sum_{k=3}^{\infty} x_{kk}\eta^k \qquad Y = \eta + \sum_{k=3}^{\infty} y_{kk}\eta^k \tag{23}$$

whose odd-indexed coefficients are given by

$$\begin{aligned} x_{kk} &= \frac{\alpha}{(\lambda^{-k}-\lambda)} \sum_{n=1}^{(k-1)/2} \frac{(-1)^n (z^{2n+1})_{kk}}{(2n+1)!(\lambda-\lambda^{-1})^{2n+1}} \simeq \frac{(-1)^{(k-1)/2}\alpha\lambda^{-k}}{k!(\lambda^{-k}-\lambda)(\lambda-\lambda^{-1})^k}[1+O(\lambda^{-3})] \\ y_{kk} &= \frac{\alpha}{(\lambda^{-k}-\lambda^{-1})} \sum_{n=1}^{(k-1)/2} \frac{(-1)^n (z^{2n+1})_{kk}}{(2n+1)!(\lambda-\lambda^{-1})^{2n+1}} \simeq \frac{(-1)^{(k-1)/2}\alpha\lambda^{-k}}{k!(\lambda^{-k}-\lambda^{-1})(\lambda-\lambda^{-1})^k}[1+O(\lambda^{-3})]. \end{aligned} \tag{24}$$

Consequently we can also resum the series (23), thus obtaining

$$\begin{aligned} X &\approx (-\alpha/\lambda^3)\eta + (\alpha/\lambda)\sin(\eta/\lambda^2) \\ Y &\approx (1-\alpha/\lambda)\eta + \alpha\lambda \sin(\eta/\lambda^2) \end{aligned} \tag{25}$$

if we neglect terms of order λ^{-2} in the coefficients. Once again we can invert the linear transformation (10) so as to obtain the approximate parametric equations for the stable manifold. However, these are simpler if we rotate the (θ, I) axes by 45°. Since we will consider the intersection of the unstable manifold with the stable manifold which converges onto the fixed point at $(2\pi, 0)$, we use the full linear transformation:

$$\theta = 2\pi + 2^{-1/2}(\theta' - I') \qquad I = 2^{-1/2}(\theta' + I'). \tag{26}$$

The stable manifold then has equations

$$\theta' = -2^{-1/2}\lambda^{-2}\eta \qquad I' \approx -2^{-1/2}[1-2(\lambda-\alpha)]\lambda^{-2}\eta + 2^{1/2}\alpha \sin(\lambda^{-2}\eta). \tag{27}$$

The homoclinic points are thus approximately given by the intersection of the two curves:

$$\begin{aligned} I &\approx [(\alpha+2)^{-1} - (\alpha+1)]\theta + \alpha \sin\theta \\ I' &\approx -3\theta' + 2^{1/2}\alpha \sin(2^{1/2}\theta') \end{aligned} \tag{28}$$

using the fact that

$$\alpha = \lambda - 2 + O(\lambda^{-1}). \tag{29}$$

They represent the unstable and stable manifolds, respectively, close to the origin. Far from the origin the terms of order λ^{-2}, which have been neglected, are multiplied by large powers of ξ or η. The simple sinusoidal form (28) eventually fails, even though the full series for the manifolds remains convergent. The problem with the series is then computational—we have to deal with very large numbers multiplied by very small

coefficients. However, all we need is to compute two distinct homoclinic points P_+ and P_- with normal coordinates $(\xi_\pm, 0)$ and $(0, \eta_\pm)$. The respective homoclinic orbits will also be linearly related, according to the first equations in (22) and (27).

For both manifolds the first sinusoidal loops have amplitudes which grow linearly with α, while the frequency of oscillation remains approximately constant. This behaviour is shown in figure 3. We obtain one homoclinic point, P_-, from the

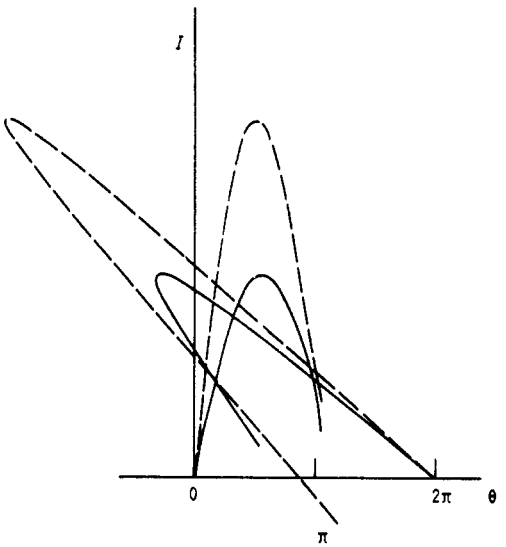

Figure 3. Homoclinic crossing for two values of $\alpha = 4$ (full curve) and 8 (broken curve) using the approximate normal form expressions (28).

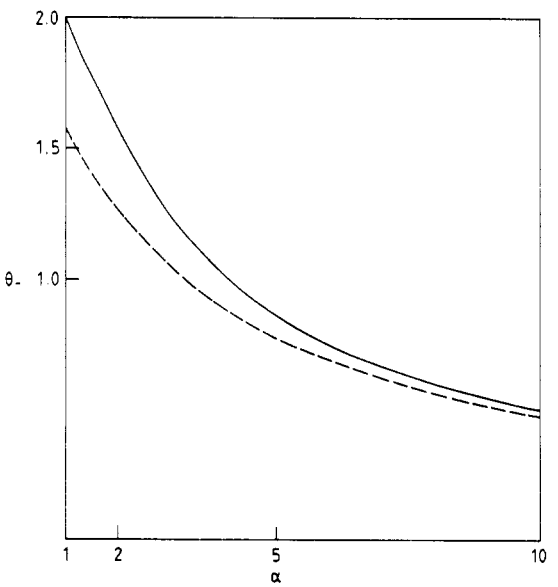

Figure 4. Behaviour of $\theta_-(\alpha)$ as computed from the normal form (full curve) and from (30) where terms of $O(\lambda^{-2})$ are neglected (broken curve).

intersection where both manifolds are approximately linear and the other, P_+, from the first return of either the stable or the unstable manifold. It is preferable to use the return of the unstable manifold, since the intersection will then occur for a smaller $\xi_+ = \lambda\theta_+$ than the η_+ obtained from the other alternative. As α becomes large we thus obtain a first approximation to the stable manifold by linearising the second equation (28). The homoclinic point P_- is then given approximately by linearising the unstable manifold around $\theta = 0$ and P_+ is obtained by linearising this manifold around $\theta = \pi$, as justified by the discussion in § 2. The result, neglecting terms $O(\lambda^{-2})$, is

$$\theta_+ = \pi \qquad \theta_- = 2\pi/(3+\alpha). \tag{30}$$

This simple approximation for θ_- is much cruder than computing the intersection of $I(\theta)$ and $I'(\theta')$ in (28), though it gives θ_+ exactly. It is also easily verified that, within the present approximation, the image of (θ_-, I_-) by the standard map has θ coordinate $2\pi - \theta_-$, as required by symmetry considerations. Figure 4 compares $\theta_-(\alpha)$ as computed directly from the normal form and from (30). The latter deviates strongly for $\alpha < 2$. In principle, we can take the normal form approximation to arbitrarily small α, but in practice we then have slow convergence as well as decreasing angles between the intersecting manifolds, leading to errors in the homoclinic point, computed in table 1 for $1 \leqslant \alpha \leqslant 9$.

4. Discommensuration energies

Truncation of the normal form provides a uniform approximation for the energy of a discommensuration. By this we mean that, besides the truncation error and the error in evaluating the phase-space coordinates of a single intersection of the stable and unstable manifolds, no more errors are introduced from the rest of the homoclinic orbit, whose θ_i coordinates are then introduced in (3). There is no other method which specifies precisely the homoclinic orbit as it accumulates on the fixed point without running into problems with exponential instability. Here, the orbit is simply given by the normal form image of $(\lambda^{-j}\xi_\pm, 0)$ and $(0, \lambda^{-i}\eta_\pm)$. These points can be computed as close to the fixed point as we like.

We can estimate the remainder of the energy on stopping at $\lambda^{-J}\xi_\pm$ in an asymptotically exact way as $J \to \infty$. To do this we note that the normal form transformation becomes the identity for $(\xi \to 0, 0)$, i.e. the homoclinic coordinates $\theta_{\pm j}$ for $j > J$ are simply obtained by inverting the linear transformation (10), taking $Y = 0$ and $X = \lambda^{-j}\xi_\pm$:

$$\theta_{\pm j} = \lambda^{-j}\xi_\pm/(1+\lambda^{-1}). \tag{31}$$

In this region we can also expand the potential about $\theta = 0$, so the energy tail is given by

$$\sum_{j=J}^{\infty} \frac{1}{2}\left(\frac{\xi_\pm}{1+\lambda^{-1}}\right)^2 [(1-\lambda)^2+\alpha]\lambda^{-2(j+1)} = \frac{\xi_\pm^2[(1-\lambda)^2+\alpha]}{(1+\lambda^{-1})^2(1-\lambda^{-2})}\lambda^{-2(J+1)}. \tag{32}$$

For large λ we need not worry about this energy tail. Indeed we need to keep only three points in the orbit of P_+ and two points on the orbit of P_-, if we neglect terms of the order of λ^{-2} as in the previous section. The soliton energy is then simply

$$\Phi_s = \frac{1}{2}\left(2\pi\frac{1+\alpha}{3+\alpha}\right)^2 + 2\alpha\left[1-\cos\left(\frac{2\pi}{3+\alpha}\right)\right] \tag{33}$$

whereas the energy corresponding to the orbit of P_+ is just

$$\Phi_m = \tfrac{1}{2}\{\pi^2 + [\lambda^{-1}\pi + \alpha \sin(\lambda^{-1}\pi)]^2\} + 2\alpha[2 - \cos(\lambda^{-1}\pi)]. \tag{34}$$

In both cases the first term is the elastic (kinetic) energy, while the second is the potential energy $\sum_i V(\theta_i)$. Note that the mass on top of the potential hump pushes up the energy, Φ_m, with slope $d\phi_m/d\alpha \to 2$ as $\alpha \to \infty$, whereas the soliton energy, Φ_s, tends to stabilise this behaviour. Figure 5 compares the exact Φ_s, computed from the normal form, with that given by (33) as well as the pinning energy $\Phi_m - \Phi_s$ computed both ways.

The third curve for the pinning energy is

$$32\pi^2 \exp(-\pi^2/\alpha^{1/2}) \tag{35}$$

derived by Pokrovsky (1981) after a series of approximations, all of which assume that $\alpha \ll 1$. Even Pokrovsky's definition of pinning energy differs from ours (Aubry's), as it measures the energy difference between the continuum approximation and the soliton. Nonetheless, Pokrovsky's ansatz works well for $\alpha \sim 10$, even though this range is so far from the continuum that two or three masses already supply a good estimate for the energies. As $\alpha \to \infty$ (35) has the wrong form, since it levels off at $32\pi^2$ instead of increasing with a slope of 2α. In this respect, Pokrovsky's alternative form

$$16\pi^2/\sinh(\pi^2/\alpha^{1/2}) \tag{36}$$

is preferable, for it increases, though only with $\alpha^{1/2}$. In both cases we are saved by the large factor π^2 and the square-root dependence on α. Thus it is only for $\alpha \sim 100$ that the exponent in (35) has a modulus of unity.

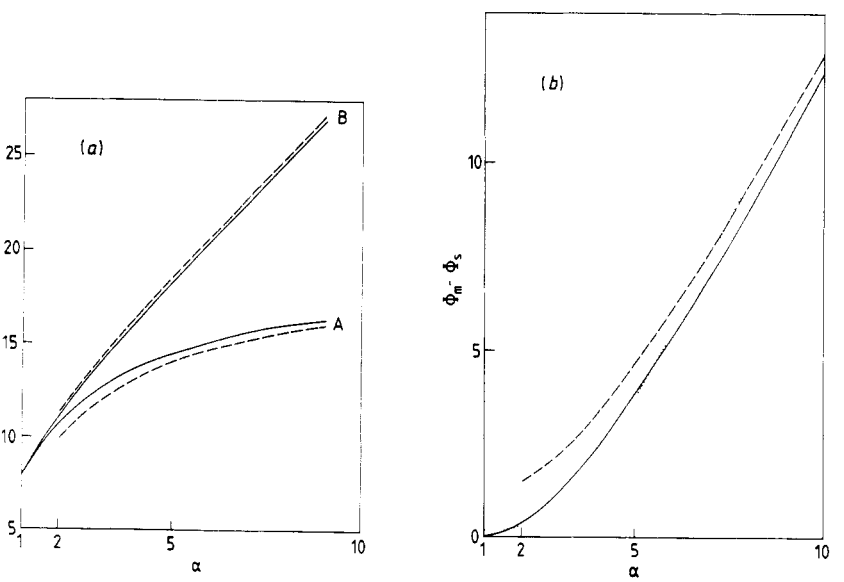

Figure 5. (*a*) Comparison of the exact (full curve) value of Φ_s(A) and Φ_m(B) computed from the normal form with that given by the approximate expression (33) and (34) (broken curve) as α varies from 1 to 9. (*b*) Comparison of the pinning energy $\Phi_m - \Phi_s$ calculated via normal form (full curve), normal form with terms of $O(\lambda^{-2})$ neglected (broken curve) and Pokrovsky's expression (dotted curve) for α in the range of 1 to 10.

5. Conclusions

The Birkhoff normal form provides analytical expressions for the stable and unstable manifold at the origin of the standard map. Truncation of the normal form provides excellent approximations to the pair of homoclinic orbits that determine the energies of a discommensuration in the Frenkel-Kontorova model. The series for the manifolds can be resummed in the limit $\alpha \to \infty$ into simple closed forms, which adequately portray their first homoclinic windings. We hence derive very simple approximations for the discommensuration energies, valid far beyond the chaotic threshold of $\alpha \sim 1$.

The agreement of the pinning energy thus computed with Pokrovsky's ansatz is a puzzle. It would be interesting to derive equivalent expressions for the discommensurations of periodic orbits of period 2, 3, ... to verify if the continuum limit still furnishes approximations which can be extrapolated into the chaotic range. More plausible is the conjecture that replacing α by $\lambda - 2$, according to (29), in the approximation for the energies may provide reasonable results for these higher discommensurations. In other words, it is possible that the energy of a discommensuration to a periodic orbit of period n depends basically on the eigenvalue λ_n of the fixed point of the nth power of the map. However, it may be that such self-similarity between homoclinic orbits only manifests itself in the limit of $n \to \infty$, as in the case of period-doubling bifurcations.

References

Aubry S 1978 *Solitons and Condensed Matter. Solid State Sciences* vol 8, ed A Bishop and T Schneider (Berlin: Springer) p 264

—— 1981 *Les Houches 1980, Physics of Defects* vol 35, ed R Balian, M Kléman and J-P Poirier (Amsterdam: North-Holland) p 431

—— 1983a *J. Physique* **44** 147

—— 1983b *Physica* **7D** 240

Aubry S and Le Daeron P 1983 *Physica* **8D** 381

Bak P 1982 *Rep. Prog. Phys.* **45** 587

Birkhoff G D 1920 *Acta Math.* **43** 1

Da Silva Ritter G L, Ozorio de Almeida A M and Douady R 1987 *Physica* D in press

De Seze L and Aubry S 1984 *J. Phys. C: Solid State Phys.* **17** 389

Lichtenberg A J and Lieberman M A 1983 *Regular and Stochastic Motion* (Berlin: Springer)

Moser J 1956 *Commun. Pure Appl. Math.* **9** 673

Ozorio de Almeida A M, Coutinho T J S E and Da Silva Ritter G L 1985 *Rev. Bras. Fis.* **15** 60

Pokrovsky V L 1981 *J. Physique* **42** 761